

Enabling an unimpeded surgical approach to the skull base in patients with cranial hyperostosis, exemplarily demonstrated for craniometaphyseal dysplasia

Technical note

PHILIPP JUERGENS, M.D., D.M.D.,^{1,2} JAVIER RATIA, M.Sc.,³ JÖRG BEINEMANN, M.D.,² ZDZISLAW KROL, D.Sc.,² KURT SCHICHO, M.D., D.Sc.,⁴ CHRISTOPH KUNZ, M.D., D.M.D., P.D.,^{1,2} HANS-FLORIAN ZEILHOFER, M.D., D.M.D.,^{1,2} AND STEPHAN ZIMMERER, M.D.⁵

¹Department of Cranio-Maxillofacial Surgery, University Hospital Basel, University of Basel;

²Hightech Research Center of Cranio-Maxillofacial Surgery, University of Basel; ³Biomaterial Science Center, University of Basel; ⁴Department of Neurosurgery, University Hospital Basel, University of Basel, Switzerland; and ⁵University Hospital of Cranio-Maxillofacial and Oral Surgery, Medical University of Vienna, Austria

Craniometaphyseal dysplasia is an extremely rare, genetic bone-remodeling disorder. Comparable to osteopetrosis, fibrous dysplasia, and other infrequent conditions, craniometaphyseal dysplasia is characterized by progressive diffuse hyperostosis of the neuro- and viscerocranium. Affected patients present with a pathognomonic dysmorphia: macrocephalus, hypertelorism, bulky facial skeleton, and a prominent mandible. Progressive thickening and petrification of the craniofacial bones can continue throughout life, often resulting in neurological symptoms due to obstruction of the cranial nerves in the foramina and therefore immediately requiring neurosurgical interventions to avoid persistent symptoms with severe impairment of function. Treatment is largely infeasible given the lack of suitable tools to perform a craniotomy through the gross calvarial bone.

In this paper, the authors present a complete process chain from the CT-based generation of an individual patient's model displaying his pathology to optimized preoperative planning of the skull's shape with a thickness of about 6–7 mm. For concise verification of the surgical plan in an operating room environment, a 3D real-time navigation prototype system was utilized. To guarantee realization of the surgery in a reasonable time frame, the mechanical tools were preoperatively selected for optimizing the ablation rate in porcine and bovine bone, which were comparable to that in the patient. This process chain was developed in a modular way, so that it could be easily adopted completely or partially for other surgical indications.

A 21-year-old man was treated according to this sophisticated concept. Skull bone more than 50 mm thick in some regions was reduced to physiological thickness. The patient was thus in a stage that neurosurgical interventions could be performed with a regular risk within a reasonable time of treatment. (DOI: 10.3171/2011.3.JNS101517)

KEY WORDS • craniometaphyseal dysplasia • genetic disease • hyperostosis • disordered bone metabolism • computer-assisted surgery • corrective surgery • intraoperative navigation • skull base

HYPEROSTOSIS of the craniofacial skeleton can be a symptom of various bone metabolism disorders. All of these diseases are very uncommon. Their infrequency makes it even more necessary to obtain consent for a treatment based on substantial diagnostics and accurate planning in affected patients.

Craniometaphyseal dysplasia is one of these extremely rare, genetic bone-remodeling conditions that can occur in an autosomal dominant or recessive form. Like osteopetrosis (Albers-Schönberg disease), fibrous dysplasia, or the Caffey syndrome, CD is characterized by progressive diffuse hyperostosis of the cranial bones.^{3,4,11,16,18} Patients clinically present with facial dysmorphia such

as a wide nasal bridge, paranasal bossing, hypertelorism with an increase in bizygomatic width, and a prominent mandible. Progressive thickening and petrification of the craniofacial bones can continue throughout life, often resulting in neurological symptoms caused by narrowing of the cranial foramina, including the foramen magnum, and therefore immediately requiring neurosurgical interventions. If untreated, compression of the cranial nerves can lead to disabling conditions such as facial palsy, facial pain, eye bulb movement disorders, blindness, and deafness (conductive and/or sensorineural hearing loss). Obstruction of the cranial vessels (carotid arteries, basilar artery, or vertebral arteries) might lead to cerebral or

Abbreviations used in this paper: CD = craniometaphyseal dysplasia; RMSE = root mean square error.

This article contains some figures that are displayed in color online but in black and white in the print edition.

Unimpeded approach to the skull base for cranial hyperostosis

cerebellar infarction with resulting neurological deficits, depending on the affected area. These effects may be mild but will most likely be severe with a disabling outcome and can even result in death. Besides the functional constraints, obvious aesthetic impairments cause suffering in patients.^{2,16,17,20,21}

In the current literature many articles on genetic conditions can be found, but the surgical treatment of this particular disease is rarely addressed.^{13,15} The few documented surgical treatment concepts focus on measures such as enlarging the foramen magnum extracranially or widening the nose cavity to allow better nasal breathing.^{8,10,25} But only the neurosurgical approach—widening of the foramina in the skull base via an intracranial approach—would be the first-choice treatment to tackle evident symptoms such as blindness, deafness, or vascular obstruction of the brain-supplying vessels. But this therapeutic option seems to be hindered given that skull bone in CD has an enormous thickness up to 50 mm or even more and that standard tools for low-risk craniotomy are unsuitable for this specific pathology. By reducing the calvarial bone to physiological thickness before a patient presents with neurological deficits, one obstacle could be overcome. Such a reduction cranioplasty is a high-risk procedure: the massive inhomogeneity of the skull bone does not allow simple reduction of a certain amount beginning on the outer bony surface and can lead to accidental injury of the dura and underlying brain tissues. Furthermore, the bone in patients with CD is much harder than usual, so that conventional tools such as chisels become dull very soon and rotating burs get hot and subsequently become damaged after only a short period of constant use. As a consequence, only a workflow that provides for exact knowledge of the individual patient's anatomy and pathology would be suitable for this kind of surgery. An accurate surgical plan, a tool for achieving the planned intervention, and instruments to guarantee an appropriate ablation rate of bone are mandatory for a reliable clinical implementation of this concept.

In this paper, we present a complete process chain starting from the CT-based generation of an individual patient's model displaying his pathology for preoperative planning, with the aim of reducing the skull to a physiological thickness of about 6–7 mm. To ensure that the preoperative plan would be precisely implemented during surgery, a 3D real-time navigation system was applied. To guarantee realization of the surgery in a reasonable time frame, the bone drills and other mechanical tools were thoroughly tested to determine their ablation and abrasion rates with high precision.

Methods

Patient History and Examination

The first clinical application of the developed treatment workflow was performed in a 21-year-old patient suffering from CD. According to his history, he exhibited noticeable hyperplasia of the neuro- and viscerocranium from early childhood, presenting typical clinical signs of the disorder. We had known the patient since he was

10 years old. At that time, we first attempted to reduce skull bone in the frontal and biparietal regions by using conventional drills and chisels. It was only possible to reduce the bone thickness by a few millimeters in 2 surgeries because of the high abrasion rate of the surgical instruments brought on by the extreme hardness of the patient's bone. After these surgeries, the patient was clinically examined every 6 months. The patient is now beyond adolescence, and a medical examination revealed the following findings: hyperplastic neuro- and viscerocranium, telecanthus, hindering of breathing through the nose, teeth irregularities, and gentle bilateral hip dysplasia (Fig. 1). Neurological deficits caused by obstruction of the foramina could not be detected via clinical examination and diagnostics including evoked potentials monitoring. Additionally, the patient presented with no signs of increased intracranial pressure, and a CT-based comparison of his intracranial volume with that of other patients of the same age showed no significant differences. Nevertheless, radiological findings revealed severe narrowing of all openings of the skull base (Fig. 2). The patient's desire for treatment was the impetus for developing a novel treatment plan. As a first step, surgical reduction of the skull bone seemed to be a reasonable procedure. Furthermore, an adaptation of the shape of the neurocranium could help the patient's appearance approximate that in the normal population. To obtain an optimal functional and aesthetic result, the patient will need additional surgeries in the future: decompression of the foramina in the skull base, if clinically indicated; correction of the telecanthus; modeling osteotomies of the viscerocranium; and/or widening of the nasal cavities. Reduction of the hyperplastic skull was chosen as the first step in this multistage treatment concept, as it would reduce the risk of any possible intervention requiring a craniotomy.

Technical Workflow

For registration of the dataset in a computer-assisted planning and navigation environment and prior to medical imaging, the patient was outfitted with 5 cortical bone screws (Synthes) in the calvarial bone while under local anesthesia. Based on a CT scan (Sensation 64, Siemens; peak kV = 120 kV, pixel spacing = [0.533203125 mm, 0.533203125 mm], and slice thickness = 1 mm), a virtual model of the patient's individual anatomy was generated. The segmentation process was performed using 2 different software packages. In the first segmentation step, commercial imaging software (Mimics 12.0, Materialise N.V.) was used to segment bony structures of the skull and to build the basis for a haptic 3D stereolithographic model. The second step was performed with the medical processing software platforms CoSegMe and SeVisMo, which were developed by us. To generate a virtual 3D model, the standard threshold-based segmentation methods, such as region growing and threshold segmentation, were applied (Fig. 3). Additional methods based on a mathematical morphology description (morphological operations: erosion, dilation, opening, and closing) were implemented as well. Significant parts of this process had to be done with manual segmentation. To smooth the ir-



Fig. 1. Photographs, frontal (left) and lateral (right) views, showing the clinical aspect of the patient prior to surgery.

regular inner surface of the bone and subsequently create a virtual bony surface with a thickness of about 6–7 mm, we used the Rapidform software package (INUS Technology, Inc.). The same program was used both to determine the local amounts of bone to be removed and to generate a distance map (Fig. 4). Because bone thickness varied between 12 and 52 mm, the skull was covered by a virtual grid of squares with an edge length of 28 mm to obtain units with restricted variations in bone thickness. Finally, the total amount of bone to be removed was calculated. Based on these calculations, drills that yielded a reasonable ablation rate were selected. The ablation rate of the mechanical tools was determined through cadaveric trials with porcine and bovine bone of comparable volumetric bone mineral density. It should be possible to perform the surgery in < 12 hours. We also tested and evaluated in advance the propulsion equipment for the drill and bone cutting tools, as these devices are not generally intended for continuous use for hours. An air-driven tool and an electrically powered device were selected (Air-Pen, E-Pen, Synthes).

To guarantee transfer of the surgical plan to the actual patient, we used a prototype 3D navigation system that we had developed. The prototype system consists of a software module (Linux-based CMF application Marvin platform, Institute for Surgical Technology and Biomechanics/Artorg Center, University of Bern, and Hightech Research Center, University of Basel) running on a laptop computer (HP Compaq 8710w mobile workstation, Hewlett Packard) equipped with accelerated 3D graphics hardware (NVIDIA Quadro FX 350M, NVIDIA Corp.) and linked via USB (universal serial bus) to serial adapter to a commercially available infrared optical tracking system (Polaris, Northern Digital, Inc.) and associated modifications to conventional instruments. The Polaris measurement system registers the position and orientation of anatomical structures and surgical instruments by measuring positions of marker spheres with a spatial ac-

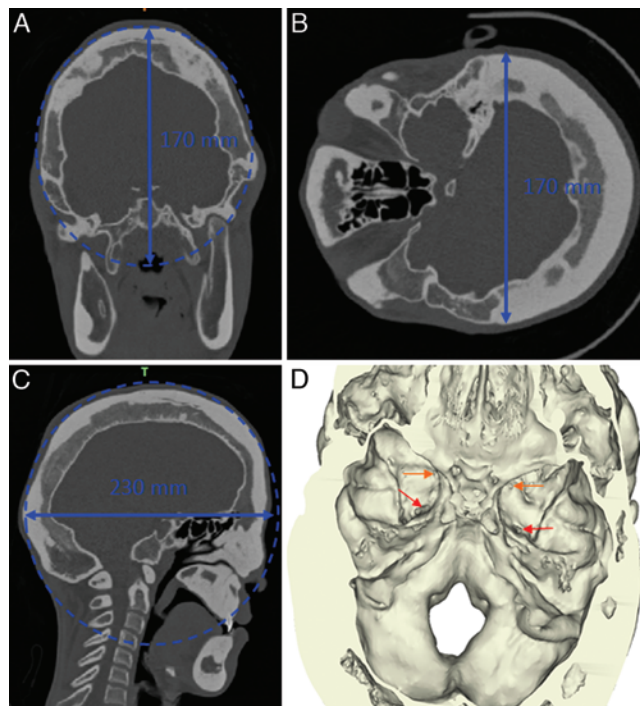


Fig. 2. Coronal (A), axial (B), and sagittal (C) thin-slice CT scans displaying hyperplastic cranial bones and a severe narrowing of foramina in the skull base region. Virtual 3D reconstruction (D) showing severe narrowing of the foramina.

curacy of 0.35 mm RMSE.^{7,14} Compared with a commercially available frameless stereotactic navigation system, our system provides real 3D navigation with an improved spatial display of the anatomical structures as well as the surgical planning. A further advantage is the possibility of a direct import of 3D planning data in an .stl file format into the navigation console.⁷

The stepwise modular configuration of the workflow is summarized in Table 1.

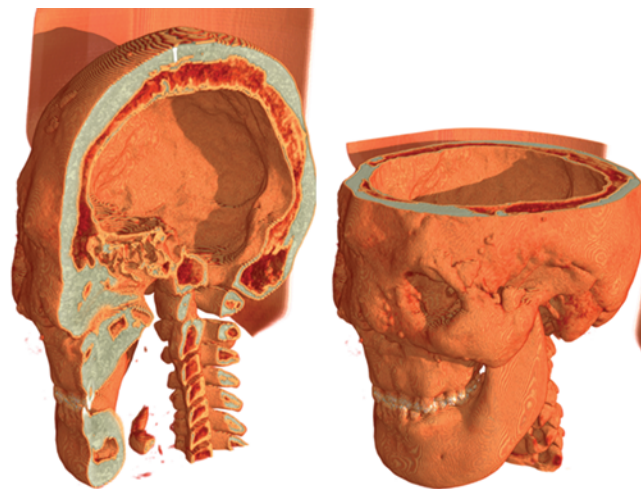


Fig. 3. Sagittal and axial virtual 3D reconstructions in volume rendering mode showing cortical and cancellous bone, whose thickness varied from 12 to 52 mm.

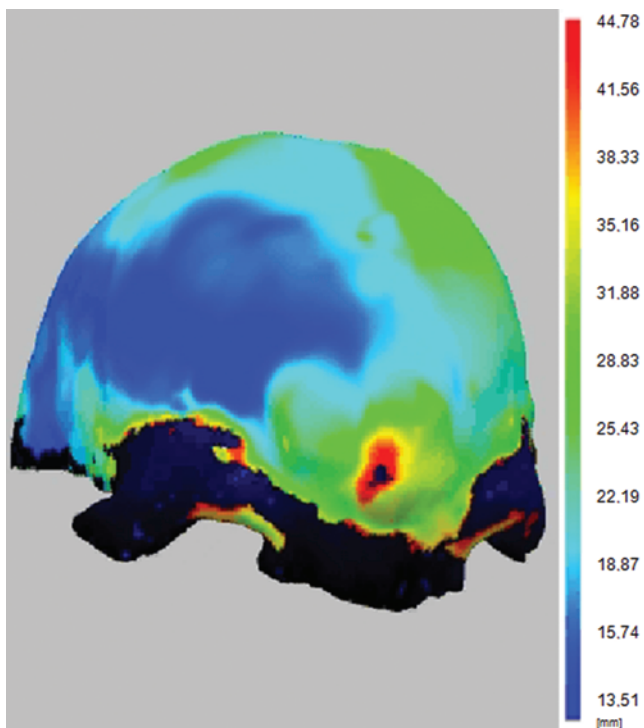


FIG. 4. Color-coded distance mapping of the virtual 3D model. Areas with less thickness are displayed in blue, areas with increased thickness in red. Regions presenting a distance between inner and outer bony surface of more than 44.8 mm appear in black.

Results

Preoperative In-Vitro Workflow Development

Application of the aforementioned software packages allowed us to generate the desired virtual bone surface. The difference between this virtual surface and the actual one provided a distance map, which formed the fundament for dividing the skull into an appropriate grid with reasonable thickness variations (Fig. 5). The thickness and orientation of the grid units determined which of the 4 selected drill-heads would be applied during the different stages of surgery—controlled depth drilling at the corner points of each square, widening of the depth drilling, connecting the corner points, and removing the remaining squares. Knowing the amount of bone to be removed and the ablation rate of the drills, featured in Table 2, the duration of the intervention was predicted with reasonable precision.

Realization of the Surgical Plan and Postoperative Outcome

After exploring the surgical site via a bicorony incision, the passive marker shields were mounted to the patient with a detachable footplate (part of the Face-O-Meter, Prof. C. Krenkel) that allows correct repositioning without losing registration. The point-to-point registration process was performed using the 5 registration screws with an accuracy of 0.4 mm RMSE (Fig. 6). After the registration process, navigation was utilized to identify the corner-points of the planned squares. Depth-controlled drillings were then performed at each corner point (Fig. 7). Directly after the preoperatively developed workflow, the corner points were connected using the flame-shaped

TABLE 1: Detailed description of the individual steps in the modular diagnostic, planning, and treatment workflow*

Step No.	Level	Process/Data Source	Description
1	basic diagnostics	CT scan, DICOM data	acquisition of CT scan of skull (Sensation 64, Siemens; peak kV = 120 kV, pixel spacing = [0.533203125 mm, 0.533203125 mm], slice thickness = 1 mm)
2	basic diagnostics	DICOM data, .stl file	generation of virtual 3D model to display patient's individual anatomy & pathology (Surgicase 5.0, Mimics 12.0, Materialise N.V./intensity-based segmentation, threshold 160–3071 HU; CoSegMe & SeVisMo, NCCR Co-ME)
3	advanced diagnostics	harvesting of bone sample	acquisition of small bone sample from It parietotemporal region of the calvarial bone under local anesthesia
4	advanced diagnostics	μ-CT scan, DICOM data	analysis of microstructure & biomechanical parameters as basis for selection of drills
5	intervention planning	.stl file	mathematical creation of new bony surface in a distance of 6–7 mm over the integrated inner cranial surface; definition of bone volume to be ablated (Rapidform, INUS Technology, Inc.)
6	intervention planning		selection of bur tips for distinct steps during the ablation process by defining their ablation rate using bovine & porcine bone specimens
7	intervention planning	.stl file	creation of a grid to segment into smaller units the area of bone to be removed; definition of distances between current & planned bony surface for depth-controlled drills on the corner points of the plan squares by using a distance mapping tool (Mimics 12.0, 3-matic 4.3, Materialise N.V.; RapidForm, INUS Technology, Inc.)
8	surgical procedure		transfer the surgical plan to the patient w/ the help of a 3D real-time navigation system
9	surgical procedure	.stl file	constant control of the ablation process w/ 3D real-time navigation system
10	evaluation	DICOM data, .stl file	superimposition of 3D virtual planning & postoperative CT scan (Mimics 12.0, Materialise N.V.)

* DICOM = Digital Imaging and Communications in Medicine.

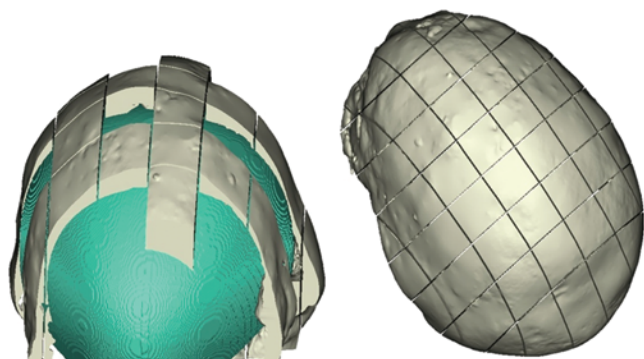


Fig. 5. Mathematically generated and optimized “new” surface in 6- to 7-mm distance to a smoothed and integrated inner bony surface (green). The virtual skull is divided into *plan squares* to allow controlled reduction of the bone into smaller units.

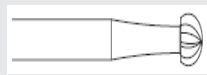
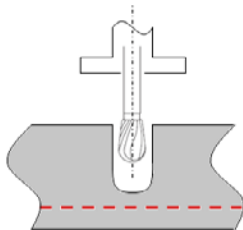
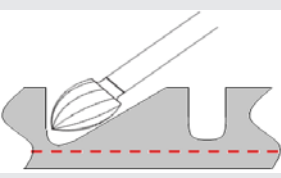
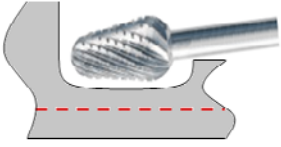
drill bit. Subsequently, the skull could be successfully reduced to the desired shape under continuous navigational control (Fig. 8). The surgery could be performed within the desired time frame of < 12 hours. Immediately post-operatively the patient was kept under intensive care for an additional 18 hours. He constantly exhibited stable vital parameters.

During the extended postoperative course, the patient exhibited excellent healing without any complication (Fig. 9). Superimposing the postoperative CT scan onto the virtual plan shows correspondence with the 3D plan (Fig. 10). The patient continues to be clinically examined every 6 months. A CT scan obtained 1 year after surgery showed no regrowth of bone in the area where the ablation was performed. Furthermore, no progressive obstruction of the foramina in the skull base could be detected.

Discussion

The presented workflow enables the accurate and straightforward reduction of skull bone in a predefined way. Our experience with this clinical case proved the durability and suitability of the surgical instruments after thorough consideration of the specifications derived from the mechanical tests and estimations. The reduction of bone thickness is the basis for potential treatments, answering esthetic as well as neurosurgical, that is, functional, criteria. We want to emphasize that the presented workflow itself can never be a stand-alone treatment option for CD. It provides the planning, surgical, and navigational tools to remodel a skull in all dimensions as a

TABLE 2: Summary of the 4 kinds of burs identified for the different steps in the surgical workflow

Image	Bur Specifications	Manufacturer	Ablation Rate (mm ³ /sec)		Task During Surgery
			Bovine	Porcine	
	round bur (ømax 8 mm)	Synthes	8–48	22–28	marking drills on edges of the squares
	pear-shaped bur (ømax 6 mm)	Synthes	14–28	27–34	 depth-controlled drilling of corner points of the grid
	acorn bur (ømax 9 mm)	Synthes	10–48	23–33	 connection of all corner points
	bur w/ cross-cut (ømax 8 mm)	Komet/Gebr. Brasseler		20–37	 reduction of the inner parts of the squares

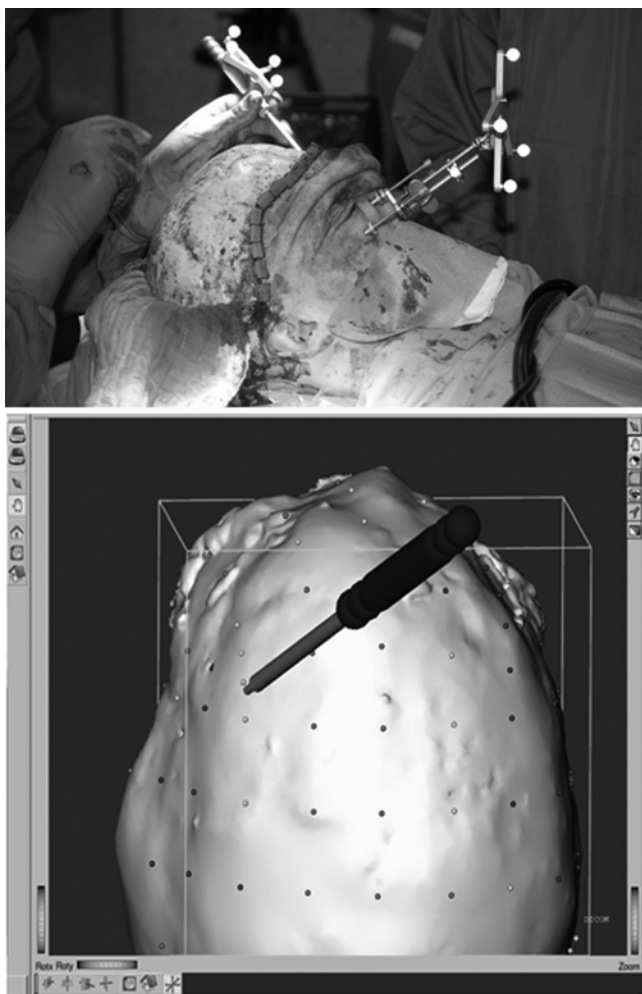


FIG. 6. Upper: Intraoperative photograph of the passive marker shields mounted on a detachable footplate (Face-o-meter, according to Prof. C. Krenkel, Salzburg, Austria) to allow removal and repositioning of the markers without losing the registration. **Lower:** Screenshot from the display of the 3D real-time navigation prototype system. The pointer-tip indicates one of the plan square corner points.

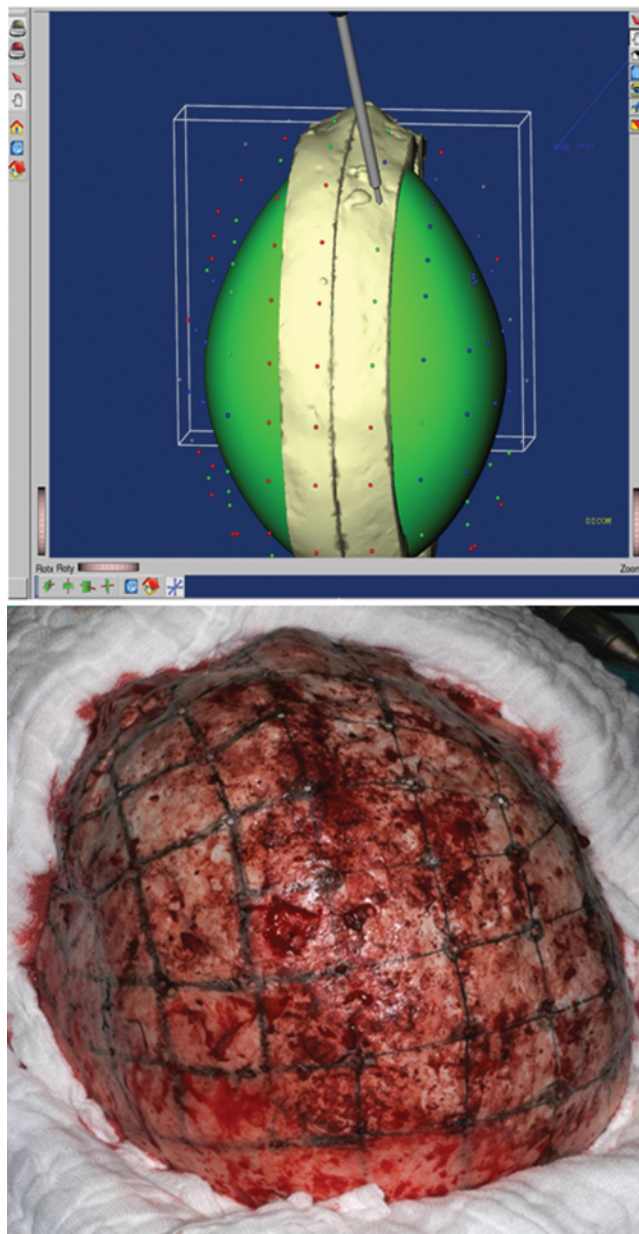


FIG. 7. Screenshot (upper) and intraoperative view (lower) showing transfer of the surgical plan to the patient.

module in a stepwise treatment chain for complex bony disorders with thickening of the skull inside and out. In patients with CD, the normalization of calvarial bone thickness is clearly more than an esthetical goal. It is a reliable approach for performing potentially life-saving intracranial neurosurgical procedures—decompression of the cranial foramina and reduction of the inner surface of the calvarial bone—within a reasonable time frame and with the use of commonly available surgical instruments in a second step. Computer-based planning and navigation controlled the precise intraoperative transfer of this surgical plan to the operating room site. Considering the inhomogeneity and variability of bone thickness typical in patients with CD is mandatory to avoid lesions of the meninges or the brain. The effort expended in terms of manpower and technical equipment to realize this surgery was relatively high. Just the identification of suitable drill bits and propulsion equipment took an engineer several weeks to perform conclusive tests on comparable bovine and porcine bone specimens. Fortunately, we were

able to use excellent infrastructure for 3D planning and intraoperative navigation techniques.

Because the planning system is built up in a modular way, it can be easily adopted for widespread use for other indications requiring corrective or even ablative surgery of the cranial vault: osteopetrosis, fibrous dysplasia, Paget disease, hyperostoting meningiomas, or other less frequent diagnoses like Proteus syndrome or conditions in which the lateral skull base is affected as in villonodular synovitis of the temporomandibular joint or Camurati-Engelmann disease.^{1,5,9,16,21–23} Especially in ablative interventions, this kind of workflow could allow future merging of the removal of bony pathologies in the anatomically and geometrically challenging region of the skull base as well as the upper viscerocranium and

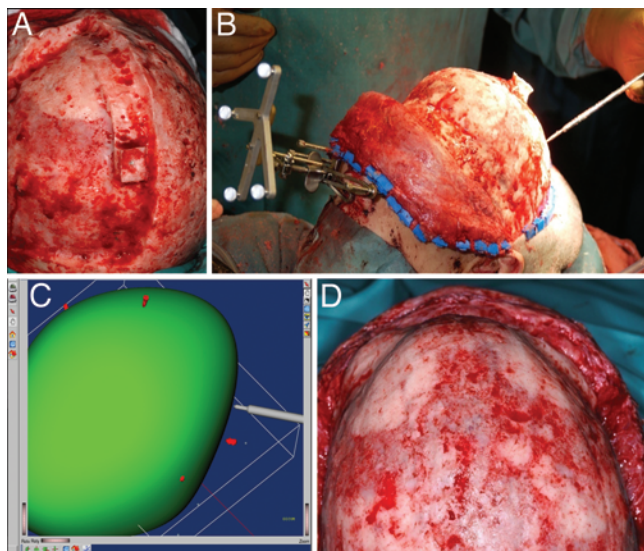


FIG. 8. Images demonstrating the stepwise reduction of calvarial bone. **A:** Situation after ablation in the left frontoparietal region (above left). In case reregistration was needed, the squares containing the marker screws were left until the end of the surgery. **B:** Pointer-tip indicating the “new” bony surface. **C:** Corresponding screenshot. **D:** Situation immediately before wound closure: the calvarial bone is ground and the supraorbital region is molded.

immediate reconstruction, for example, in patients with specific alloplastic implants.^{6,24}

The recorded CT data for the preoperative planning, visualization, simulation, and navigation are the baseline for follow-up diagnostics. The first follow-up diagnostic was done 1 year after the bone resection to exclude any changes in the area of the surgical field as well as in the skull base region and foramen magnum. The patient is regularly examined every 6 months and he will undergo further CT studies after 3 years, unless a neurological deficit or subjective changes occur. This wait-and-see approach was chosen because of the substantial side effects of foramen magnum decompression via suboccipital craniectomy and C-1 and C-2 laminectomy combined with dural augmentation, as they are described in the literature.^{10,25} As a consequence, we see no reason to perform any kind of prophylactic or preventive intracranial surgery either in the foramen magnum region or at the skull base until we register any neurological deficiency. The aspect of genetic predisposition, whether the CD is autosomal dominant or autosomal recessive, does not influence the decision to perform surgery or adopt a wait-and-see strategy. The autosomal dominant type is characterized by facial distortion and cranial nerve compression.^{11,12,19,26} The autosomal recessive type is characterized by an even more extensive form of sclerosis of the cranial bones than is the autosomal dominant type.¹⁷ In both types there is no need for functional treatment as long as the patient is without symptoms: our approach prepares affected patients for any neurosurgical intracranial approaches needed. Besides the functional aspects, it is obvious that the patient also benefits from an aesthetic improvement via normalization of the shape of the cranium. If no neurological impairment occurs, the next surgical steps



FIG. 9. Photographs of the patient 12 days after surgery.

in our patient will be dedicated to improving his facial appearance: a reduction of the cheek bones, correction of the telecanthus, correction of the nasal skeleton, and reduction of the bony overgrowth in the mandible. These efforts will be undertaken to allow the patient better social integration, knowing that a potentially life-saving neurosurgical intervention could be performed now with a lower risk.

Conclusions

The presented workflow is a safe method of normalizing the shape of calvarial bone in patients with thickening bony disorders as a modular step in the treatment of, for example, CD. It can serve as a first step in a multistage surgical treatment of affected patients. Our experience shows that patients and surgeons clearly benefit from the intensive use of planning in an interdisciplinary team with engineers. The gathered results are germane to all concepts in which neurosurgical intracranial approaches in such patients are needed, especially to reach the skull base region. The workflow can also apply to all other indications for which bone thickening of the cranial skull should be treated in a safe and predictable way.

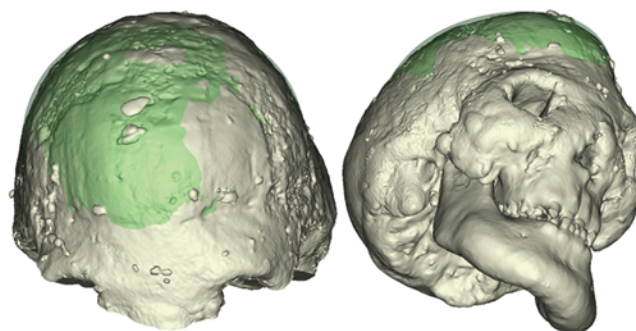


FIG. 10. Three-dimensional reconstructions of the postoperative CT scan superimposed on the virtual plan demonstrates excellent matching between corresponding data sets. *Green* indicates the planning, *light gray*, the postoperative CT scan.

Unimpeded approach to the skull base for cranial hyperostosis

Disclosure

This work was supported by the National Center of Competence in Research, Computer Aided and Image Guided Medical Interventions (NCCR CO-ME) of the Swiss National Science Foundation, Bern, Switzerland.

Author contributions to the study and manuscript preparation include the following. Conception and design: Juergens, Ratia, Beinemann, Zeilhofer. Acquisition of data: Juergens, Ratia, Beinemann, Krol, Kunz, Zeilhofer. Analysis and interpretation of data: Juergens, Ratia, Krol, Zeilhofer. Drafting the article: Schicho. Critically revising the article: Ratia, Schicho, Zimmerer. Approved the final version of the paper on behalf of all authors: Juergens. Administrative/technical/material support: Juergens, Ratia, Beinemann, Krol, Kunz, Zeilhofer. Study supervision: Zeilhofer.

Acknowledgment

The authors extend special thanks to Prof. Dr. Bert Mueller of the Biomaterials Science Centre, University of Basel, for providing laboratory resources and the manpower to perform the cadaveric trials and to select the propulsion engine most suitable for our purposes.

References

1. Adolphs N, Tinschert S, Bier J, Klein M: Craniofacial hyperostoses in Proteus syndrome—a case report. **J Craniomaxillofac Surg** **32**:391–394, 2004
2. Ahmad FU, Mahapatra AK, Mahajan H: Craniofacial surgery for craniometaphyseal dysplasia. **Neurol India** **54**:97–99, 2006
3. Caffey J: Infantile cortical hyperostoses. **J Pediatr** **29**:541–559, 1946
4. Caffey J: Infantile cortical hyperostosis; a review of the clinical and radiographic features. **Proc R Soc Med** **50**:347–354, 1957
5. Carlson ML, Beatty CW, Neff BA, Link MJ, Driscoll CL: Skull base manifestations of Camurati-Engelmann disease. **Arch Otolaryngol Head Neck Surg** **136**:566–575, 2010
6. Chacón-Moya E, Gallegos-Hernández JF, Piña-Cabrales S, Cohn-Zurita F, Goné-Fernández A: Cranial vault reconstruction using computer-designed polyetheretherketone (PEEK) implant: case report. **Cir Cir** **77**:437–440, 2009
7. Chapuis J, Schramm A, Pappas I, Hallermann W, Schwenzler-Zimmerer K, Langlotz F, et al: A new system for computer-aided preoperative planning and intraoperative navigation during corrective jaw surgery. **IEEE Trans Inf Technol Biomed** **11**:274–287, 2007
8. Cheung VG, Boechat MI, Barrett CT: Bilateral choanal narrowing as a presentation of craniometaphyseal dysplasia. **J Perinatol** **17**:241–243, 1997
9. Day JD, Yoo A, Muckle R: Pigmented villonodular synovitis of the temporomandibular joint: a rare tumor of the temporal skull base. **J Neurosurg** **109**:140–143, 2008
10. Day RA, Park TS, Ojemann JG, Kaufman BA: Foramen magnum decompression for cervicomedullary encroachment in craniometaphyseal dysplasia: case report. **Neurosurgery** **41**:960–964, 1997
11. Dhar SU, Taylor T, Trinh C, Sutton VR: Cranio-meta-diaphyseal dysplasia: 25 year follow-up and review of literature. **Am J Med Genet A** **152A**:2335–2338, 2010
12. Elçioglu N, Hall CM: Temporal aspects in craniometaphyseal dysplasia: autosomal recessive type. **Am J Med Genet** **76**:245–251, 1998
13. Iughetti P, Alonso LG, Wilcox W, Alonso N, Passos-Bueno MR: Mapping of the autosomal recessive (AR) craniometaphyseal dysplasia locus to chromosome region 6q21-22 and confirmation of genetic heterogeneity for mild AR spondylocostal dysplasia. **Am J Med Genet** **95**:482–491, 2000
14. Juergens P, Krol Z, Zeilhofer HF, Beinemann J, Schicho K, Ewers R, et al: Computer simulation and rapid prototyping for the reconstruction of the mandible. **J Oral Maxillofac Surg** **67**:2167–2170, 2009
15. Kornak U, Brancati F, Le Merrer M, Lichtenbelt K, Höhne W, Tinschert S, et al: Three novel mutations in the ANK membrane protein cause craniometaphyseal dysplasia with variable conductive hearing loss. **Am J Med Genet A** **152A**:870–874, 2010
16. Kusano T, Hirabayashi S, Eguchi T, Sugawara Y: Treatment strategies for fibrous dysplasia. **J Craniofac Surg** **20**:768–770, 2009
17. Lamazza L, Messina A, D'Ambrosio F, Spink M, De Biase A: Craniometaphyseal dysplasia: a case report. **Oral Surg Oral Med Oral Pathol Oral Radiol Endod** **107**:e23–e27, 2009
18. Mandl ES, Buis DR, Heimans JJ, Peerdeman SM: Acquired encephaloceles and epilepsy in osteopetrosis. **Acta Neurochir (Wien)** **149**:79–81, 2007
19. McKay DR, Fialkov JA: Autosomal dominant craniometaphyseal dysplasia with atypical features. **Br J Plast Surg** **55**:144–148, 2002
20. Mintz S, Velez I: Craniometaphyseal dysplasia associated with obstructive sleep apnoea syndrome. **Dentomaxillofac Radiol** **33**:262–266, 2004
21. Mirsadeghi SM, Meybodi AT, Nejat F, Saberi H: Bilateral jugular foraminal stenosis in a patient with benign osteopetrosis associated with pseudotumor cerebri syndrome. Case report. **J Neurosurg** **110**:804–807, 2009
22. Park BY, Cheon YW, Kim YO, Pae NS, Lee WJ: Prognosis for craniofacial fibrous dysplasia after incomplete resection: age and serum alkaline phosphatase. **Int J Oral Maxillofac Surg** **39**:221–226, 2010
23. Sakamoto Y, Nakajima H, Kishi K, Shimizu R, Nakajima T: Management of craniofacial hyperostosis in Proteus syndrome. **J Craniofac Surg** **21**:414–418, 2010
24. Scolozzi P, Martinez A, Jaques B: Complex orbito-fronto-temporal reconstruction using computer-designed PEEK implant. **J Craniofac Surg** **18**:224–228, 2007
25. Sewell MD, Akram H, Wadley J: Foramen magnum decompression and expansile duroplasty for acquired Chiari type I malformation in craniometaphyseal dysplasia. **Br J Neurosurg** **22**:83–85, 2008
26. Tinschert S, Braun HS: Craniometaphyseal dysplasia in six generations of a German kindred. **Am J Med Genet** **77**:175–181, 1998

Manuscript submitted September 7, 2010.

Accepted March 21, 2011.

Please include this information when citing this paper: published online April 15, 2011; DOI: 10.3171/2011.3.JNS101517.

Address correspondence to: Philipp Juergens, M.D., D.M.D., Department of Cranio-Maxillofacial Surgery, University Hospital Basel, University of Basel, Spitalstrasse 21, 4031 Basel, Switzerland. email: pjuergens@uhbs.ch.